Journal of Hepatocellular Carcinoma

Dovepress
open access to scientific and medical research

Open Access Full Text Article

ORIGINAL RESEARCH

CXCL9 Overexpression Predicts Better HCC Response to Anti-PD-1 Therapy and Promotes N1 Polarization of Neutrophils

Pei Wang[1,2,*], Ming-Hao Xu[3,*], Wen-Xin Xu[3,*], Zi-Ying Dong[4], Ying-Hao Shen[3], Wen-Zheng Qin[1]

[1]Endoscopy Center and Endoscopy Research Institute, Zhongshan Hospital, Fudan University, Shanghai, 200032, People's Republic of China; [2]Department of Digestive Medicine, Wuwei People's Hospital, Wuwei City, Gansu Province, 733000, People's Republic of China; [3]Department of Liver Surgery and Transplantation, Liver Cancer Institute and Zhongshan Hospital, Fudan University, Shanghai, 200032, People's Republic of China; [4]Department of CT/MRI Center, Wuwei People's Hospital, Wuwei City, Gansu Province, 733000, People's Republic of China

*These authors contributed equally to this work

Correspondence: Wen-Zheng Qin, Endoscopy Center and Endoscopy Research Institute, Zhongshan Hospital, Fudan University, Shanghai, 200032, People's Republic of China, Tel/Fax +86-21-64041990, Email qin.wenzheng@zs-hospital.sh.cn; Ying-Hao Shen, Department of Liver Surgery and Transplantation, Liver Cancer Institute and Zhongshan Hospital, Fudan University, No. 180, Fenglin Road, Shanghai, 200032, People's Republic of China, Tel/Fax +86-21-64041990, Email syh12268@163.com

Background: Anti-programmed death-1 (PD1) antibodies have changed the treatment landscape for hepatocellular carcinoma (HCC) and exhibit promising treatment efficacy. However, the majority of HCCs still do not respond to anti-PD-1 therapy.

Methods: We analyzed the expression of CXCL9 in blood samples from patients who received anti-PD-1 therapy and evaluated its correlation with clinicopathological characteristics and treatment outcomes. Based on the results of Cox regression analysis, a nomogram was established for predicting HCC response to anti-PD-1 therapy. qRT–PCR and multiple immunofluorescence assays were utilized to analyze the proportions of N1-type neutrophils in vitro and in tumor samples, respectively.

Results: The nomogram showed good predictive efficacy in the training and validation cohorts and may be useful for guiding clinical treatment of HCC patients. We also found that HCC cell-derived CXCL9 promoted N1 polarization of neutrophils in vitro and that AMG487, a specific CXCR3 inhibitor, significantly blocked this process. Moreover, multiple immunofluorescence (mIF) showed that patients with higher serum CXCL9 levels had greater infiltration of the N1 phenotype of tumor-associated neutrophils (TANs).

Conclusion: Our study highlights the critical role of CXCL9 as an effective biomarker of immunotherapy efficacy and in promoting the polarization of N1-type neutrophils; thus, targeting the CXCL9-CXCR3 axis could represent a novel pharmaceutical strategy to enhance immunotherapy for HCC.

Keywords: CXCL9, anti-PD-1 antibody, N1 polarization of neutrophils, nomogram

Introduction

Hepatocellular carcinoma (HCC) is the most common type of liver cancer and is often diagnosed at advanced stages when surgical resection is contraindicated.[1] Therefore, systemic treatment is the main treatment option for patients with advanced HCC. Standard first-line treatment options for HCC typically include sorafenib, lenvatinib, and other kinds of immunotherapy. In addition, combination treatment regimens have shown promising results. Atezolizumab in combination with bevacizumab is now recommended based on the IMbrave150 Phase III trial results.[2,3] Other combinations, such as targeted therapy combined with immunotherapy or immunotherapy combined with antiangiogenic drugs, are being rigorously evaluated for their efficacy and adverse effects in large clinical trials.[4] In theory, due to the different mechanisms of action of two drugs in a combination therapy, synergistic effects can be exerted to maximize the antitumor benefits. Moreover, toxicity is not additive.[5] In addition, with the advancements in systematic treatment, neoadjuvant therapy and adjuvant therapy for HCC have also received increasing amounts of attention.[6] The postoperative adjuvant atezolizumab combined with bevacizumab has also

Received: 30 November 2023
Accepted: 18 February 2024
Published: 8 May 2024

been proven to prolong the progression-free survival of HCC patients.[7] The PD-1/PD-L1 pathway represents a key immune checkpoint that tumors utilize to evade immune surveillance. Thus, blockade of the PD-1/PD-L1 pathway has revolutionized cancer immunotherapy, leading to significant improvements in patient outcomes across multiple tumor types, including HCC.[8] PD-1 inhibitors, such as nivolumab[9] and pembrolizumab,[10] have shown promising activity in the treatment of HCC. These agents restore the function of T cells, unleashing the immune system on tumors and leading to durable tumor responses in advanced HCC. However, not all HCCs respond equally to anti-PD-1 therapy. The MOUSEION-01 study suggested that the benefit of single-agent immunotherapy versus the control treatment was less pronounced in female patients than in male patients.[11] Thus, there is an unmet need for effective predictive markers to guide individualized treatment.

In recent years, the role of chemokines in HCC has gained increasing attention. Along with their receptors, chemokines, a family of small signaling proteins, are expressed in various tissues and organs, including the liver. Evidence suggests that chemokines regulate the growth, invasion, and metastasis of HCC cells.[12] Several chemokines have been identified as potential biomarkers for liver cancer diagnosis and prognosis. For instance, high levels of C-reactive protein (CRP), a protein produced by the liver in response to inflammation, have been associated with poor prognosis in HCC patients who received combination therapy comprising atezolizumab and bevacizumab.[13] According to a large-scale retrospective analysis, elevated baseline serum interleukin-8 (IL-8) levels are associated with poor outcomes in patients with advanced cancer treated with nivolumab and/or ipilimumab, everolimus or docetaxel in Phase 3 clinical trials.[14] Chemokines can promote the proliferation and survival of HCC cells by activating downstream signaling cascades. They can also facilitate the invasion and metastasis of tumor cells by regulating the expression of matrix metalloproteinases (MMPs) and other proteolytic enzymes.[15] Additionally, chemokines can modulate the tumor microenvironment by recruiting immune cells and stromal cells to support tumor growth and progression.[16] Targeting chemokines to treat HCC represents a novel therapeutic approach. Blocking the function of specific chemokines or their receptors can effectively interfere with tumor growth and metastasis. Some inhibitors of chemokine receptors have shown promise in preclinical studies,[17] while others are currently being evaluated in clinical trials for the treatment of liver cancer. The development of such targeted therapies offers hope for patients with liver cancer, particularly those who do not respond to conventional treatments.

Tumor-associated neutrophils (TANs) are a subset of neutrophils that are recruited to the tumor microenvironment and interact with cancer cells in various ways. In liver cancer, TANs can polarize into protumorigenic N1-like or tumor-suppressing N2-like phenotypes. N1-like TANs are proinflammatory and promote tumor growth through the release of proangiogenic and prometastatic factors. On the other hand, N2-like TANs have anti-inflammatory properties and can inhibit tumor growth by releasing antiangiogenic and proapoptotic factors.[18] The interaction between TANs and HCC cells is regulated by various signaling pathways, including cytokines, chemokines, and growth factors. Understanding these interactions and the mechanisms that regulate TAN polarization in liver cancer can provide insights into the development of more effective therapeutic strategies.[17]

In the present study, based on transcriptome sequencing results from multiple centers, we found that the chemokine CXCL9 is associated with anti-PD-1 therapy in HCC patients. Moreover, we further developed a comprehensive predictive model that relies solely on serum and clinical indicators to predict HCC response to anti-PD-1 therapy and demonstrated that this model has considerable specificity and sensitivity in a validation cohort. We also explored for the first time the direct relationship between CXCL9 and N1-type TAN polarization in HCC, which will provide further insights into the influence of the TME via CXCL9.

Materials and Methods

Patients and Samples

The present study cohort comprised 211 patients treated with anti-PD-1 antibody for unresectable or advanced HCC at our medical center between January 2019 and January 2023. The diagnosis of HCC was based on typical imaging findings obtained via abdominal contrast-enhanced computed tomography (CT) or magnetic resonance imaging (MRI). After excluding patients who did not complete at least 6 months of therapy (n = 28), 183 patients were ultimately included in the analysis. The criteria for treatment were Barcelona Clinic Liver Cancer (BCLC) stage C or BCLC stage B disease with a physical state exceeding tolerance of interventional therapy. Patients received 200 mg of anti-PD-1

antibody every 3 weeks. Tumor response was evaluated every 2 months according to the Response Evaluation Criteria in Solid Tumors (RECIST) v1.1. Progression free survival (PFS) was defined as the time from the initiation of systemic treatment to disease progression.

The study protocol complied with the ethical guidelines of the World Medical Association Declaration of Helsinki and was approved by the Wuwei People's Hospital Research Ethics Committee. Written informed consent was obtained from the patients before initiation of anti-PD-1 therapy.

Enzyme-Linked Immunosorbent Assay (ELISA) and Quantitative Real-Time PCR (qRT–PCR)

Serum CXCL9 concentrations were determined using an ELISA kit (R&D Systems, Inc., Minneapolis, MN) according to the manufacturer's instructions. The expression levels of CD95, NOS2, CCL3, CD206, ARG2 and CCL2 were measured via qRT–PCR. Supplementary Table 1 shows the sequences of primers used. Total RNA was extracted from neutrophils using TRIzol reagent (Takara). After employing 1 μg of total RNA and the PrimeScript RT Reagent Kit (Takara), cDNA was synthesized. The mRNA levels were subsequently determined via qRT–PCR using the SYBR Green Master Mix Kit (Yeasen).

Cell Isolation and Culture

Peripheral blood samples from people in normal health were collected in EDTA-coated tubes. Neutrophils were isolated using the MojoSort™ Whole Blood Human Neutrophil Isolation Kit (Cat. 480152, Biolegend). Primary HCC cells were collected using gentleMACS™ Dissociators according to the manufacturer's instructions. Briefly, tumor tissue ranging from 0.05–0.2 g was dissociated in 2.5 mL of an enzyme mixture. The sample was incubated for 30 minutes at 37 °C under continuous rotation using the MACSmix™ Tube Rotator. The sample was resuspended, and the cell suspension was applied to a MACS SmartStrainer (30 μm or 70 μm) placed in a 50 mL tube. The cell suspension was centrifuged at 300×g for 7 minutes. The supernatant was aspirated completely. The cells were resuspended as needed for coculture.

The obtained cells were resuspended in DMEM supplemented with 10% fetal bovine serum and penicillin and streptomycin.

Multiple Immunofluorescence (mIF)

For mIF, the slides were deparaffinized in xylene, rehydrated in ethanol, incubated with 0.3% hydrogen peroxide, subjected to antigen retrieval with citrate buffer, and blocked with 5% BSA. Primary antibodies were incubated overnight at 4 °C, followed by incubation with a secondary horseradish peroxidase-conjugated antibody. The slides were again placed in citrate buffer to remove redundant antibodies before the next step. Finally, the slides were incubated with DAPI solution at 37 °C for 10 min in the dark. Finally, the slides were scanned and analyzed with Case Viewer.

Transwell Migration Assay of Neutrophils

Briefly, the isolated neutrophils were resuspended in serum-free RPMI-1640 medium containing 1% P/S at a concentration of 10^6/mL. Then, in the presence of LPS (300 ng/mL), 200 μL of cells was seeded into the upper wells of the Transwell chamber (8 μm; Corning, NY, USA). Thereafter, the medium from the upper chamber containing HCC cells with high or low CXCL9 secretion was collected, centrifuged to remove floating cells, and placed in the lower chamber. After 2 hours, the number of cells that migrated to the bottom chamber was counted using a hemocytometer.

Statistical Analysis

Continuous variables are presented as the means ± SEMs and were compared using the Mann–Whitney *U*-test (Wilcoxon rank-sum test) or Student's *t*-test. Categorical variables were compared using Fisher's exact test or the chi-square test, as appropriate. PFS was plotted using the Kaplan–Meier method and compared using the Log rank test. Two-tailed p values of < 0.05 were considered to indicate statistical significance. All the statistical analyses were conducted with R software (v3.6.3; R Project for Statistical Computing).

Results

HCCs in Patients with Higher Serum CXCL9 Levels Exhibit Improved Response to Anti-PD-1 Treatment

To identify effective biomarkers of the response to anti-PD-1 therapy, we reanalyzed the transcriptome sequence of 111 tumor samples from patients with advanced HCC from 13 centers before systemic anti-PD-1 therapy. Compared with those of nonresponders, the transcriptome analysis of responders revealed a significant upregulation in CXCL9 ($p < 0.01$) (Figure 1A).[19] As CXCL9 is a potential chemokine that is present in the tumor microenvironment and blood circulation, the serum CXCL9 concentration in each patient was measured in the training cohort from our center (n=123) treated with anti-PD-1 antibody. We found that patients with a partial response (PR) had the highest baseline serum CXCL9 levels, followed by patients with stable disease (SD), while patients with progressive disease (PD) had the lowest serum CXCL9 levels (Figure 1B and Figure S1A and B). Based on the association between CXCL9 and response to anti-PD-1 therapy, we calculated a cutoff value of 478 pg/mL for the serum CXCL9 concentration (AUC=0.7999; specificity=68.49%, sensitivity=78.00%) (Figure 1C). Further analysis revealed that a majority of patients with a serum CXCL9 concentration lower than the upper limit of the cutoff value (ULC) had PD, while patients with a serum CXCL9 concentration higher than 2x the ULC had more PR or SD (Supplementary Table 2) (Figure 1D). The baseline characteristics of the 123 patients included based on their serum CXCL9 concentrations are presented in Table 1. Consistently, Kaplan–Meier analysis suggested that patients with a serum CXCL9 concentration higher than 2x ULC had the best progression-free survival (PFS), while patients with a serum CXCL9 concentration lower than the ULC had the worst PFS (mPFS (<ULC): 11.5 months; mPFS (ULC~2x ULC): 33 months; mPFS (>2x ULC): 36.5 months; $p < 0.001$) (Supplementary Table 3) (Figure 1E); the results of the pairwise comparison can be found in Supplementary Table 3. Therefore, the serum CXCL9 concentration may serve as a novel predictor of the response to anti-PD-1 therapy.

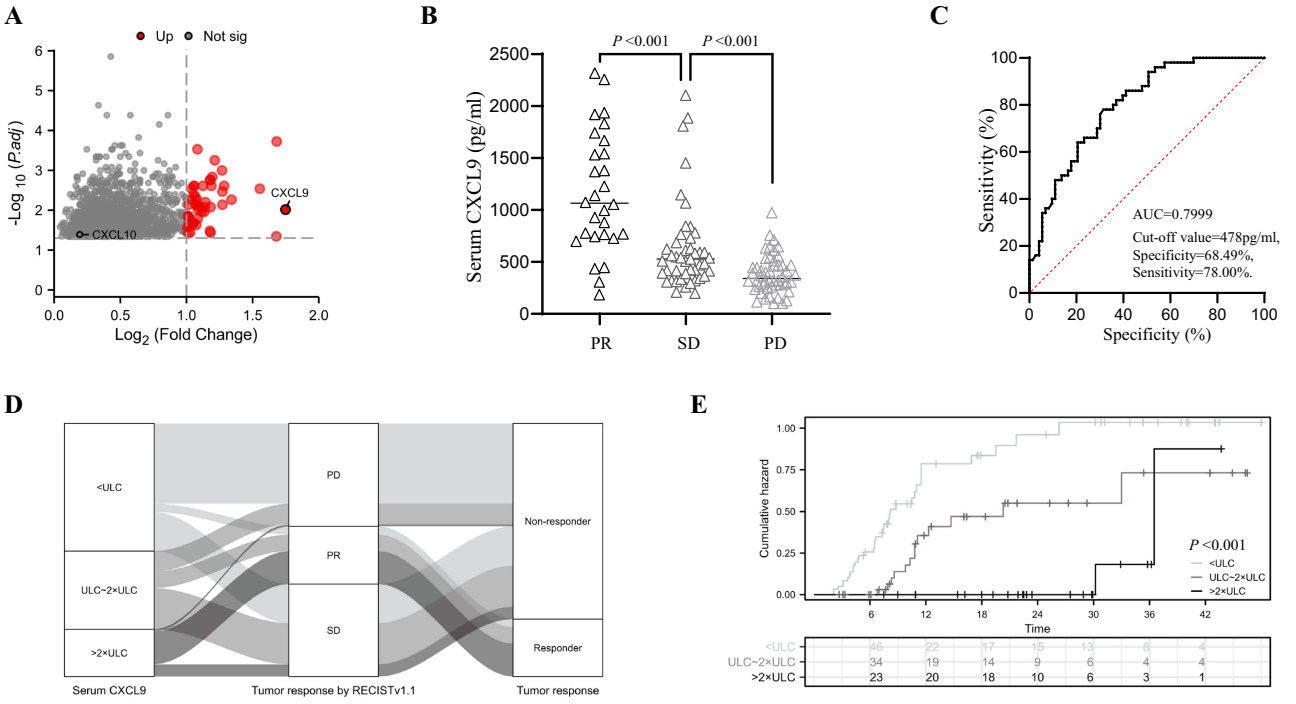

Figure 1 Patients with higher serum CXCL9 levels show a better treatment response to anti-PD-1 therapy. (**A**) Volcano plots showing the genes differentially expressed between responders and nonresponders. The most significantly expressed gene, CXCL9, is highlighted in red. (**B**) Serum CXCL9 levels in patients with PR, SD and PD HCC. (**C**) ROC curves for the response to anti-PD-1 therapy plotted according to the serum CXCL9 concentration. (**D**) Sankey analysis of serum CXCL9 levels and tumor response according to Response Evaluation Criteria in Solid Tumors (RECIST) v1.1. (**E**) PFS of patients with a serum CXCL9 concentration < ULC, 1~2x ULC or >2x ULC. **Abbreviations**: PD-1, programmed death-1; PR, partial response; SD, stable disease; PD, progressive disease; HCC, hepatocellular carcinoma; ROC, receiver operating characteristic; AUC, area under curve; ULC, upper limit of the cutoff value.

Table 1 Baseline Characteristics of Patients with Different Serum CXCL9 Levels

Characteristic	<ULC	ULC~2×ULC	>2×ULC	P value
n	62	38	23	
Age, years, mean ± sd	64.581 ± 8.8068	62.579 ± 9.5171	62.304 ± 10.412	0.457
Tumor burden, cm, n (%)				0.286
<10	35 (28.5%)	21 (17.1%)	17 (13.8%)	
>10	27 (22%)	17 (13.8%)	6 (4.9%)	
Tumor number, n (%)				0.776
Multiple	19 (15.4%)	10 (8.1%)	8 (6.5%)	
Single	43 (35%)	28 (22.8%)	15 (12.2%)	
Sex, n (%)				0.153
Male	51 (41.5%)	36 (29.3%)	21 (17.1%)	
Female	11 (8.9%)	2 (1.6%)	2 (1.6%)	
BCLC stage, n (%)				0.060
B	17 (13.8%)	7 (5.7%)	1 (0.8%)	
C	45 (36.6%)	31 (25.2%)	22 (17.9%)	
Metastasis, n (%)				0.580
No	45 (36.6%)	24 (19.5%)	15 (12.2%)	
Yes	17 (13.8%)	14 (11.4%)	8 (6.5%)	
Child–Pugh class, n (%)				0.733
A	61 (49.6%)	37 (30.1%)	23 (18.7%)	
B	1 (0.8%)	1 (0.8%)	0 (0%)	
ECOG, n (%)				0.423
1	15 (12.2%)	12 (9.8%)	5 (4.1%)	
0	45 (36.6%)	23 (18.7%)	18 (14.6%)	
2	2 (1.6%)	3 (2.4%)	0 (0%)	
HBsAg, n (%)				0.832
Positive	50 (40.7%)	32 (26%)	18 (14.6%)	
Negative	12 (9.8%)	6 (4.9%)	5 (4.1%)	
HBV-DNA, n (%)				0.700
Positive	29 (23.6%)	21 (17.1%)	12 (9.8%)	
Negative	33 (26.8%)	17 (13.8%)	11 (8.9%)	
AFP, ng/mL, n (%)				0.633
20~400	9 (7.3%)	6 (4.9%)	2 (1.6%)	
>400	34 (27.6%)	16 (13%)	11 (8.9%)	
<20	19 (15.4%)	16 (13%)	10 (8.1%)	
CEA, ng/mL, median (IQR)	2.2 (1.6, 3.925)	2.75 (2.2, 4.475)	3.1 (1.7, 4.65)	0.262
TB, μmol/L, median (IQR)	14.6 (10.575, 19.075)	14.35 (10.725, 20.575)	16.1 (11.85, 22.85)	0.539
ALB, g/L, mean ± sd	37.968 ± 4.089	38.342 ± 4.6631	41.217 ± 5.0178	0.011
SII, median (IQR)	791.5 (447.62, 1350.9)	614.33 (431.51, 957.33)	442.93 (305.5, 959)	0.050
PLR, median (IQR)	165.78 (118.94, 230.74)	164.44 (98.306, 198.94)	114 (83.872, 154.2)	0.009
NLR, median (IQR)	5.3667 (3.8409, 7.4875)	4.5528 (3.7056, 6.9886)	4.1429 (2.2873, 5.9621)	0.238
MLR, median (IQR)	1.1143 (0.8264, 1.4794)	0.88167 (0.64479, 1.0795)	0.85556 (0.59509, 1.1511)	0.017

Notes: Categorical variables are summarized as n (%). Continuous variables are summarized as medians (ranges).

Abbreviations: AFP, α-fetoprotein; ALB, albumin; BCLC, Barcelona Clinic Liver Cancer; CEA, carcinoembryonic antigen; ECOG PS, Eastern Cooperative Oncology Group performance status; HBsAg, hepatitis B surface antigen; IQR, interquartile range; MLR, monocyte-to-lymphocyte ratio; NLR, neutrophil-to-lymphocyte ratio; PLR, platelet-to-lymphocyte ratio; SII, systemic immune-inflammation index; TB, total bilirubin; ULC, upper limit of the cutoff value.

Establishment of the Nomogram for Predicting the Response to Anti-PD-1 Therapy

Further analysis was performed to explore which baseline features were also associated with immunotherapy response of HCC. The results of univariate analysis are shown in Table 2. Specifically, the independent factors predictive of the response to anti-PD-1 therapy were the serum CXCL9 concentration, tumor burden, albumin (ALB) level, systemic immune-inflammation index (SII), and platelet-to-lymphocyte ratio (PLR) (Table 2). These independent risk factors were included in the establishment of the nomogram for the response to anti-PD-1 therapy (Figure 2A). Receiver operating

Table 2 Variables Associated with the Response to Anti-PD-1 Therapy in the Training Cohort

Characteristic	Total(N)	Univariate Analysis		Multivariate Analysis	
		Hazard Ratio (95% CI)	P value	Hazard Ratio (95% CI)	P value
Serum CXCL9, pg/mL	123				
<ULC	62	Reference		Reference	
ULC~2×ULC	38	3.407 (0.879–13.208)	0.076	3.909 (0.971–15.742)	0.055
>2×ULC	23	8.266 (2.365–28.892)	**< 0.001**	7.902 (2.117–29.494)	**0.002**
Age, years	123	0.989 (0.947–1.033)	0.627		
Tumor burden, cm	123				
<10	73	Reference		Reference	
>10	50	0.428 (0.179–1.021)	0.056	0.245 (0.087–0.688)	**0.008**
Tumor number	123				
Multiple	37	Reference			
Single	86	1.005 (0.450–2.248)	0.989		
Sex	123				
Male	108	Reference			
Female	15	0.914 (0.214–3.898)	0.903		
BCLC stage	123				
B	25	Reference			
C	98	2.000 (0.684–5.848)	0.206		
Metastasis	123				
No	84	Reference			
Yes	39	1.468 (0.607–3.553)	0.394		
ECOG PS	123				
1	32	Reference			
0	86	2.030 (0.698–5.900)	0.194		
2	5	0.000 (0.000 - Inf)	0.998		
HBsAg	123				
Positive	100	Reference			
Negative	23	0.732 (0.274–1.956)	0.533		
HBV-DNA	123				
Positive	62	Reference			
Negative	61	0.630 (0.291–1.364)	0.241		
AFP, ng/mL	123				
<20	45	Reference			
20~400	17	0.921 (0.253–3.353)	0.901		
>400	61	1.561 (0.695–3.504)	0.281		
CEA, ng/mL	123	0.883 (0.730–1.067)	0.198		
TB, μmol/L	123	0.994 (0.960–1.029)	0.726		
ALB, g/L	123	1.090 (1.005–1.182)	**0.038**	1.026 (0.932–1.130)	0.598
SII	123	0.998 (0.996–1.000)	**0.017**	0.999 (0.997–1.002)	0.648
PLR	123	0.985 (0.976–0.995)	**0.002**	0.987 (0.976–0.999)	**0.027**
NLR	123	0.899 (0.783–1.031)	0.128		
MLR	123	0.466 (0.173–1.252)	0.130		

Note: Bold font, P<0.05.

Abbreviations: AFP, α-fetoprotein; ALB, albumin; BCLC, Barcelona Clinic Liver Cancer; CEA, carcinoembryonic antigen; CI, confidence interval; ECOG PS, Eastern Cooperative Oncology Group performance status; HBsAg, hepatitis B surface antigen; MLR, monocyte-to-lymphocyte ratio; NLR, neutrophil-to-lymphocyte ratio; PLR, platelet-to-lymphocyte ratio; SII, systemic immune-inflammation index; TB, total bilirubin; ULC, upper limit of the cutoff value.

characteristic (ROC) curve analysis, decision curve analysis (DCA) and calibration curve analysis (CCA) were adopted to assess the predictive accuracy of the nomogram. The area under the ROC curve was 0.959 (95% CI=0.925–0.993) for the nomogram, 0.931 (95% CI=0.887–0.975) for the SII-PLR-ALB-tumor burden score, 0.724 (95% CI=0.627–0.821) for the SII score and 0.796 (95% CI=0.728–0.864) for the PLR score (Figure 2B). Moreover, DCA and CCA suggested

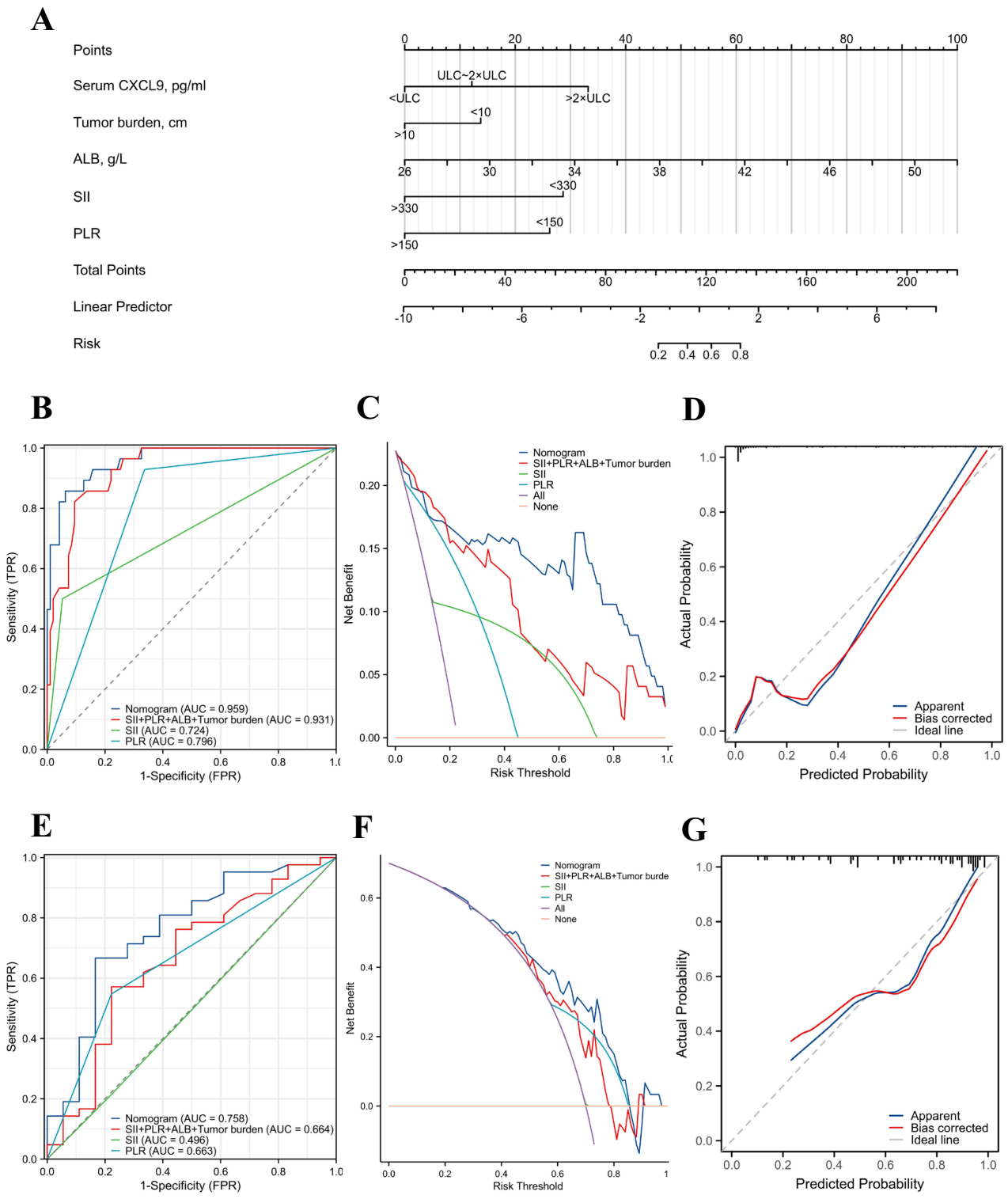

Figure 2 Establishment of the nomogram for predicting the response to anti-PD-1 therapy (**A**) Nomogram for the prediction of the response of HCC to anti-PD-1 antibody in the training cohort. B. ROC curves for the nomogram in the training cohort (**B**) and external validation cohort (**E**). Decision curves for the nomogram in the training cohort (**C**) and external validation cohort (**F**). Calibration curves for the nomogram in the training cohort (**D**) and validation cohort (**G**).
Abbreviations: ROC, receiver operating characteristic; AUC, area under curve; SII, immune-inflammation index; PLR, platelet-to-lymphocyte ratio.

the ideal predictive value of the nomogram (Figure 2C and D). The model was further evaluated in a validation cohort. The training cohort and the validation cohort differed significantly only in terms of the MLR, so the two groups were considered comparable (Table 3). The area under the ROC curve was 0.758 (95% CI, 0.618–0.898), 0.664 (95% CI,

Table 3 Comparison of the Baseline Characteristics Between the Training and Validation Cohorts

Characteristic	Training Cohort	Validation Cohort	P value
n	123	60	
Serum CXCL9, pg/mL, n (%)			0.133
>2×ULC	23 (12.6%)	18 (9.8%)	
ULC~2×ULC	38 (20.8%)	20 (10.9%)	
<ULC	62 (33.9%)	22 (12%)	
Age, years, median (IQR)	65 (57.5, 70)	64 (57, 68)	0.372
Tumor burden, cm, n (%)			0.239
<10	73 (39.9%)	41 (22.4%)	
>10	50 (27.3%)	19 (10.4%)	
Tumor number, n (%)			0.656
Multiple	37 (20.2%)	20 (10.9%)	
Single	86 (47%)	40 (21.9%)	
Sex, n (%)			0.162
male	108 (59%)	48 (26.2%)	
female	15 (8.2%)	12 (6.6%)	
BCLC stage, n (%)			0.473
C	98 (53.6%)	45 (24.6%)	
B	25 (13.7%)	15 (8.2%)	
Metastasis, n (%)			0.350
Yes	39 (21.3%)	15 (8.2%)	
No	84 (45.9%)	45 (24.6%)	
Child–Pugh class, n (%)			0.814
A	121 (66.1%)	60 (32.8%)	
B	2 (1.1%)	0 (0%)	
ECOG PS, n (%)			0.302
1	33 (18%)	14 (7.7%)	
0	86 (47%)	46 (25.1%)	
2	4 (2.2%)	0 (0%)	
HBsAg, n (%)			0.050
Positive	100 (54.6%)	41 (22.4%)	
Negative	23 (12.6%)	19 (10.4%)	
HBV-DNA, n (%)			0.185
Positive	62 (33.9%)	24 (13.1%)	
Negative	61 (33.3%)	36 (19.7%)	
AFP, ng/mL, n (%)			0.072
20~400	17 (9.3%)	11 (6%)	
<20	45 (24.6%)	30 (16.4%)	
>400	61 (33.3%)	19 (10.4%)	
CEA, ng/mL, median (IQR)	2.7 (1.8, 4.35)	2.4 (1.775, 4.825)	0.728
TB, μmol/L, median (IQR)	14.7 (10.75, 20.85)	14.45 (10.475, 21.575)	0.664
ALB, g/L, mean ± sd	38.691 ± 4.5828	40.067 ± 4.8812	0.064
SII, median (IQR)	655.5 (403.1, 1083.8)	755.92 (386.23, 1297.2)	0.650
PLR, median (IQR)	154.55 (107.67, 218.04)	138.88 (90.929, 248.75)	0.418
NLR, median (IQR)	5.1667 (3.75, 6.9773)	4.0455 (2.7612, 7.3143)	0.117
MLR, median (IQR)	0.98571 (0.72111, 1.3667)	0.67222 (0.39417, 1.2)	< 0.001

Notes: Categorical variables are summarized as n (%). Continuous variables are summarized as medians (ranges).
Abbreviations: AFP, α-fetoprotein; ALB, albumin; BCLC, Barcelona Clinic Liver Cancer; CEA, carcinoembryonic antigen; ECOG PS, Eastern Cooperative Oncology Group performance status; HBsAg, hepatitis B surface antigen; IQR, interquartile range; MLR, monocyte-to-lymphocyte ratio; NLR, neutrophil-to-lymphocyte ratio; PLR, platelet-to-lymphocyte ratio; SII, systemic immune-inflammation index; TB, total bilirubin; ULC, upper limit of the cutoff value.

0.505–0.823), 0.496 (95% CI, 0.379–0.613), and 0.663 (95% CI, 0.538–0.787) for the nomogram, the SII-PLR-ALB-tumor burden score, the SII score and the PLR score, respectively, in the validation cohort (Figure 2E). Consistent with the training cohort, the validation cohort demonstrated a high net benefit of the nomogram according to the DCA curves (Figure 2F). The calibration curve showed consistency between the predictions and observations in the validation cohort (Figure 2G).

Risk Stratification of the Nomogram

The nomogram score corresponding to the maximum Youden index was considered the cutoff value in the training cohort. Patients with a nomogram score higher than 107.6 were considered high response group to anti-PD-1 therapy, and those with a lower nomogram score were considered low response group. Based on these findings, we pooled the probabilities of response to anti-PD-1 therapy for different risk groups in the training cohort and the validation cohort (Table 4). HCC in patients in the high-risk group demonstrated a significantly higher frequency of response to anti-PD-1 therapy than those in the low-risk group, which was demonstrated in the training cohort and the validation cohort ($p < 0.001$, $p = 0.004$; respectively). Therefore, the CXCL9-based predictive nomogram we constructed may be clinically useful for selecting appropriate treatment strategies for HCC patients.

Tumor-Derived CXCL9 Promotes N1 Polarization of Neutrophils Through CXCR3

Given the potential role of CXCL9 as a cytokine in the remodeling of the TME, we speculated that the association of CXCL9 with the anti-PD-1 response in HCC is likely related to its impact on the immune microenvironment. We then used the ssGSEA algorithm in the TCGA database to calculate the infiltration of various immune cells in patients with high and low CXCL9 expression and performed correlation analysis using Pearson and Spearman correlations. We found that high expression of CXCL9 is associated with the infiltration of various immune cells, including natural killer (NK) cells, dendritic cells (DCs), T cells, macrophages and neutrophils (Figure S2A). CXCL9 has been repeatedly reported to be secreted by the DC-NK axis, mediating antigen presentation in HCC and other tumor models,[20,21] and Ruben Bill et al demonstrated that macrophage polarity can be defined by CXCL9 and SPP1 expression but not by conventional M1 and M2 markers, with a noticeably strong prognostic association. A study of $CXCL9^{+}$ macrophage polarity revealed a highly coordinated network of either pro- or antitumor variables that involved each tumor-associated cell type and was spatially organized.[22] This finding is consistent with our analysis results. In addition, we observed a significant increase in the infiltration level of neutrophils in patients with high CXCL9 expression (Figure S2B), which was further validated by in vitro Transwell migration assay (Figure S3A). There have been few previous studies on CXCL9 and neutrophils in liver cancer, so we were curious whether CXCL9 can directly act on neutrophils or whether complex immune regulation causes increased levels of neutrophil infiltration. In addition, the level of neutrophil infiltration seems to be associated with poor prognosis in patients with liver cancer,[23] which contradicts the role of CXCL9 that we previously discovered. Therefore, we hypothesized that CXCL9 may activate the antitumor phenotype of neutrophils. After culturing neutrophils in vitro and detecting markers of neutrophil polarization, we observed that treatment of neutrophils with CXCL9 significantly increased the expression of the N1 polarity markers CD95, NOS2, and CCL3 (Figure 3A) while decreasing

Table 4 Incidence of Response to Anti-PD-1 Therapy in the High-Risk Group and Low-Risk Group in the Training Cohort and Validation Cohort

Cohort	Subgroup	Response	*P* value
Training cohort	High response group	24(80)	*P* < 0.001
	Low response group	4(4.3)	
Validation cohort	High response group	12(52.2)	*P* = 0.004
	Low response group	6(16.2)	

Note: Variables are summarized as n (%).

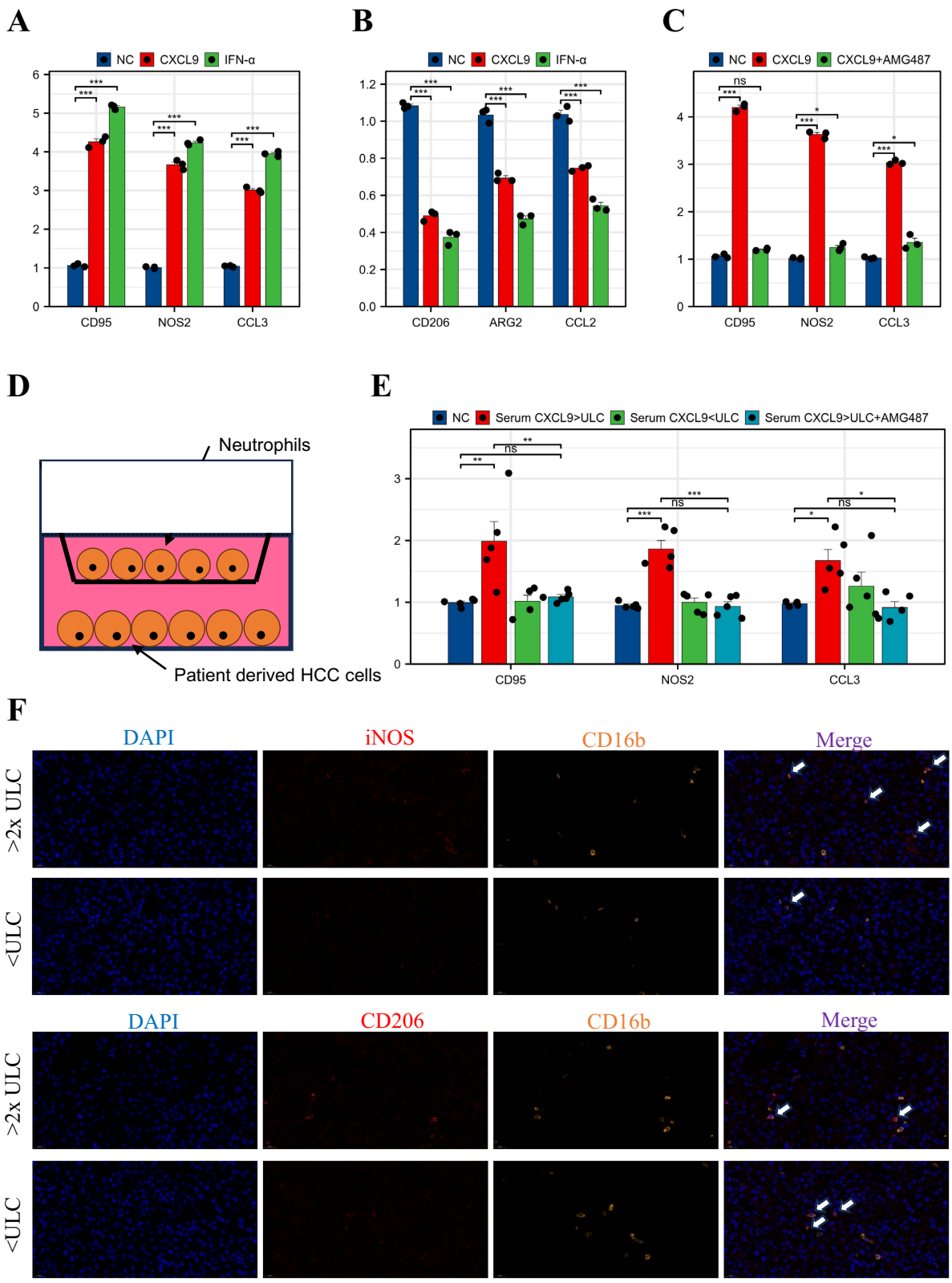

Figure 3 Tumor-derived CXCL9 promotes N1 polarization of neutrophils through CXCR3. (**A** and **B**) qPCR analysis of the transcription of N1 and N2 markers in neutrophils treated with or without recombinant human CXCL9 and IFN-α. (**C**) qPCR analysis of the transcription of N1 markers in neutrophils treated with or without AMG487. (**D**) Schematic diagram of the coculture of neutrophils and patient-derived HCC cells. (**E**) qPCR analysis of the transcription of N1 markers in neutrophils cocultured with designated patient-derived HCC cells. (**F**) Representative mIHC images of stained $CD206^{+}CD16b^{+}$ cells and $iNOS^{+}CD16b^{+}$ cells from the high- and low-CXCL9 groups. *P < 0.05; **P<0.01; ***P<0.001.

Abbreviation: ns, not significant.

the expression of the N2 polarity markers CD206, ARG2, and CCL2 (Figure 3B). CXCR3 has been reported to be the receptor for CXCL9 in TANs.[24] Blocking the CXCR3 receptor with AMG487, a CXCR3-specific inhibitor, abolished the polarization effect of CXCL9 (Figure 3C). These findings demonstrated that CXCL9 can promote the N1 polarization of neutrophils through the CXCR3 axis. CXCL9 is secreted by immune cells, endothelial cells, and tumor cells.[25] The present study screened for CXCL9 based on transcriptome data from tumor cells, so we were curious whether CXCL9 from tumor cells could promote neutrophil polarization. Tumor cells from patients with high and low serum CXCL9 levels were extracted and cocultured with neutrophils for 6 hours in a Transwell system to avoid direct physical contact (Figure 3D), after which the marker levels of the neutrophils were again detected. We found that tumor cells from patients with high CXCL9 expression promoted N1 polarization of neutrophils, and this process was inhibited by AMG487 (Figure 3E). The in vitro results demonstrated that tumor-derived CXCL9 can promote neutrophil N1 polarization through the CXCR3 axis in a paracrine manner.

A Higher Serum CXCL9 Concentration is Correlated with More N1-Type TANs in HCC Tumor Samples

mIF was used to examine the level of neutrophil infiltration in the tumor tissues of HCC patients. $CD206^{+}CD16b^{+}$ cells were considered to be N1-type TANs, while $iNOS^{+}CD16b^{+}$ cells were considered to be N2-type TANs.[26] In three patients with serum CXCL9 levels below the ULC and three patients with serum CXCL9 levels above the 2x ULC, we noticed that higher serum CXCL9 levels were associated with more N1 neutrophil infiltration, further confirming our in vitro results (Figure 3F and Figure S4A and B).

Discussion

Although immunotherapy, which includes anti-PD-1 antibodies, has achieved exciting results in the treatment of advanced HCC, the nonresponsiveness of a considerable number of HCCs in clinical practice has limited the overall therapeutic efficacy in treating this disease. Therefore, researchers have made great efforts to find effective biomarkers to predict the efficacy of immunotherapy. Hyung-Don Kim et al reported that HCCs with a discrete population of PD1-high CD8+ T cells express TIM3 and/or LAG3 and produce low levels of IFNG and TNF in response to anti-CD3 therapy. HCCs with a discrete population of PD1-high CD8+ T cells might be more susceptible to combined immune checkpoint blockade-based therapies.[27] Shi et al proposed a correlation between specific tumor immune features and anti-PD-1 therapy using single-cell techniques, which may facilitate early diagnosis and novel immunotherapy for patients with HCC.[28] In the present study, we conducted a secondary analysis of the sequencing results from multicenter studies in the United States and Europe and found that CXCL9 was the most highly expressed molecule. As a chemokine, CXCL9 has been reported to have a chemotactic effect. Jack Y Lee et al demonstrated that CXCL9 treatment reshaped the tumor microenvironment to promote dendritic cell licensing and CD8+ T-cell activation in melanoma and provided concomitant benefit to patients receiving anti-PD-1 therapies.[29] One study suggested that blocking CXCR3 signaling exacerbates tumor growth in mice, while intratumoral injection of recombinant CXCL9/10 plus intraperitoneal injection of an anti-PD-1 antibody inhibits tumor growth in mice.[30] However, there is currently no research suggesting a relationship between the serum CXCL9 concentration and immunotherapy efficacy. In the present study, a risk model based on the serum CXCL9 concentration was proven to accurately predict HCC response to immunotherapy. With respect to the validation cohort, the model also demonstrated a very high level of prediction ability. The present study has great potential because it can estimate the response of HCC to immunotherapy using a simple peripheral blood test, which is very attractive to clinicians. Although the accuracy of this model still needs improvement, stratification into different risk groups could benefit patient and physician treatment choices. In the future, additional indicators and more accurate and effective predictive factors will inevitably be identified, allowing the quick and easy identification of patients suitable for immunotherapy.

We also screened other baseline parameters related to treatment response, including a decreased tumor burden, increased serum ALB concentration, and decreased serum SII and PLR values. Notably, multiple studies have reported that the SII and PLR are associated with treatment response and that these values significantly predict the prognosis of patients with HCC after curative resection and TACE.[31,32] In another study at our center, an SII $\geq$ 330 was significantly associated with vascular

invasion, large tumors, and early recurrence. CTC counts were significantly greater in the SII ≥ 330 subgroup than in the other subgroup.[33] Therefore, the cutoff value of the SII in the present study was consistent with their result of an SII ≥ 330. The predictive effect of the SII or PLR during immunotherapy is also well explained. A lower SII may indicate that neutrophils can activate endothelial cells and parenchymal cells, enhancing the adhesive force of circulating tumor cells and promoting distal metastasis of tumors. Neutrophils can also release inflammatory factors such as neutrophil elastase, matrix metalloproteinase 9, and IL-8 to participate in tumor proliferation and metastasis.[34] In addition, platelets can directly activate the nuclear factor κB and TGF-β/Smad signal transduction pathways in tumor cells, induce epithelial-to-mesenchymal transition, and promote distal metastasis of tumor cells. Platelets can also serve as a protective "cloak" to shield circulating tumor cells from immune destruction, playing a key role in tumor cell survival and metastasis.[35] Lymphocytes can induce cytotoxic cell death and cytokine secretion, inhibit tumor cell proliferation and migration, and control tumor growth. Additionally, lower lymphocyte counts are associated with a lower survival rate in cancer patients, likely due to the weakening of the host's anticancer immunity as lymphocyte levels decrease.[36]

TANs from HCC have been found to play dual roles in tumor development and progression; for example, some studies have reported their protumorigenic activities, while others have suggested their tumor-suppressing potential.[37,38] TANs are recruited to the tumor microenvironment through the release of chemoattractants by cancer cells or other stromal cells. Once recruited, TANs can interact with liver cancer cells through direct cell–cell contact or through the release of soluble factors. These interactions can either promote or inhibit tumor growth, depending on the specific context and TAN polarization status.[39] Targeting TANs in liver cancer is a potential approach for cancer treatment. Strategies to modulate TAN function or interactions with liver cancer cells have attracted much attention. Jack Leslie et al reported that CXCR2 inhibition during immunotherapy for nonalcoholic steatohepatitis (NASH)-HCC was accompanied by an unexpected increase in tumor-associated neutrophils (TANs), which switched from a protumor to an antitumor progenitor-like neutrophil phenotype.[40] An acidic/photosensitive DC-based neoantigen nanovaccine has been explored for its ability to remodel tumor-associated neutrophils to potentiate the anticancer immune response and enhance immunotherapy efficacy.[41] Moreover, CXCL6 and TGF-β secreted by HCC cells activate extracellular signal-regulated kinase (ERK) 1/2 signaling in CAFs to increase CLCF1 production, thus forming a positive feedback loop to accelerate HCC progression. Inhibition of CLCF1/ciliary neurotrophic factor receptor signaling efficiently impaired N2 polarization of TANs both in vitro and in vivo.[42] CXCL9 has been reported to promote the infiltration of immune cells in different cancers. In this study, we investigated the role of CXCL9 in promoting neutrophil infiltration and directly promoting neutrophil polarization toward the N1 phenotype in a paracrine manner. Tumor samples were also collected to evaluate the presence of TANs in patients receiving anti-PD-1 therapy to validate our results. The results suggested that high serum CXCL9 levels were associated with increased N1 neutrophil infiltration and predicted improved immunotherapy response. Our results suggest that the exogenous introduction of CXCL9 promotes N1 polarization in neutrophils, while the inhibition of CXCR3 significantly blocks this process. Although additional evidence is still needed, our study provides a novel target for altering neutrophil phenotypes.

Conclusion

Our findings suggest that the serum CXCL9-based risk model may serve as a potential criterion for clinical decision-making related to HCC immunotherapy and provide a new approach for improving the efficacy of anti-PD-1 therapy. Targeting the CXCL9/CXCR3 axis represents a novel strategy for cancer immunotherapy by promoting N1 polarization of neutrophils and restoring their antitumoral activity.

Data Sharing Statement

Data are available from the authors upon reasonable request.

Ethics Approval and Consent to Participate

The study protocol complied with the ethical guidelines of the World Medical Association Declaration of Helsinki and was approved by the Zhongshan Hospital Research Ethics Committee. Written informed consent was signed by the patients before treatment.

Author Contributions

All the authors made a significant contribution to the work reported, whether it was in the study conception, study design, execution, acquisition of data, analysis and interpretation of data, or all of these areas; took part in drafting, revising or critically reviewing the article; gave final approval of the version to be published; agreed on the journal to which the article was submitted; and agreed to be accountable for all aspects of the work.

Funding

This study was funded by the National Natural Science Foundation of China (Grant No. 82172799).

Disclosure

The authors report no conflicts of interest in this work

References

1. Yang JD, Hainaut P, Gores GJ, Amadou A, Plymoth A, Roberts LR. A global view of hepatocellular carcinoma: trends, risk, prevention and management. *Nat Rev Gastroenterol Hepatol*. 2019;16(10):589–604. doi:10.1038/s41575-019-0186-y
2. Finn RS, Qin S, Ikeda M, et al. Atezolizumab plus bevacizumab in unresectable hepatocellular carcinoma. *N Engl J Med*. 2020;382(20):1894–1905. doi:10.1056/NEJMoa1915745
3. Rizzo A, Ricci AD, Brandi G. Atezolizumab in advanced hepatocellular carcinoma: good things come to those who wait. *Immunotherapy*. 2021;13(8):637–644. doi:10.2217/imt-2021-0026
4. Rizzo A, Ricci AD, Brandi G. Immune-based combinations for advanced hepatocellular carcinoma: shaping the direction of first-line therapy. *Future Oncol*. 2021;17(7):755–757. doi:10.2217/fon-2020-0986
5. Zhu XD, Sun HC. Emerging agents and regimens for hepatocellular carcinoma. *J Hematol Oncol*. 2019;12(1):110. doi:10.1186/s13045-019-0794-6
6. Rizzo A, Ricci AD, Brandi G. Systemic adjuvant treatment in hepatocellular carcinoma: tempted to do something rather than nothing. *Future Oncol*. 2020;16(32):2587–2589. doi:10.2217/fon-2020-0669
7. Qin S, Chen M, Cheng AL, et al. Atezolizumab plus bevacizumab versus active surveillance in patients with resected or ablated high-risk hepatocellular carcinoma (IMbrave050): a randomised, open-label, multicentre, phase 3 trial. *Lancet*. 2023;402(10415):1835–1847.
8. Ruf B, Heinrich B, Greten TF. Immunobiology and immunotherapy of HCC: spotlight on innate and innate-like immune cells. *Cell Mol Immunol*. 2021;18(1):112–127. doi:10.1038/s41423-020-00572-w
9. Yau T, Park JW, Finn RS, et al. Nivolumab versus sorafenib in advanced hepatocellular carcinoma (CheckMate 459): a randomised, multicentre, open-label, phase 3 trial. *Lancet Oncol*. 2022;23(1):77–90. doi:10.1016/S1470-2045(21)00604-5
10. Finn RS, Ryoo BY, Merle P, et al. Pembrolizumab as second-line therapy in patients with advanced hepatocellular carcinoma in KEYNOTE-240: a randomized, double-blind, phase III trial. *J Clin Oncol*. 2020;38(3):193–202. doi:10.1200/JCO.19.01307
11. Santoni M, Rizzo A, Mollica V, et al. The impact of gender on The efficacy of immune checkpoint inhibitors in cancer patients: the MOUSEION-01 study. *Crit Rev Oncol Hematol*. 2022;170:103596. doi:10.1016/j.critrevonc.2022.103596
12. Zajkowska M, Mroczko B. Chemokines in primary liver cancer. *Int J Mol Sci*. 2022;23(16):8846. doi:10.3390/ijms23168846
13. Hatanaka T, Kakizaki S, Hiraoka A, et al. Prognostic impact of C-reactive protein and alpha-fetoprotein in immunotherapy score in hepatocellular carcinoma patients treated with atezolizumab plus bevacizumab: a multicenter retrospective study. *Hepatol Int*. 2022;16(5):1150–1160. doi:10.1007/s12072-022-10358-z
14. Schalper KA, Carleton M, Zhou M, et al. Elevated serum interleukin-8 is associated with enhanced intratumor neutrophils and reduced clinical benefit of immune-checkpoint inhibitors. *Nat Med*. 2020;26(5):688–692. doi:10.1038/s41591-020-0856-x
15. Shen C, Li J, Li R, et al. Effects of Tumor-Derived DNA on CXCL12-CXCR4 and CCL21-CCR7 axes of hepatocellular carcinoma cells and the regulation of sinomenine hydrochloride. *Front Oncol*. 2022;12:901705. doi:10.3389/fonc.2022.901705
16. Ozga AJ, Chow MT, Luster AD. Chemokines and the immune response to cancer. *Immunity*. 2021;54(5):859–874. doi:10.1016/j.immuni.2021.01.012
17. Pang N, Shi J, Qin L, et al. IL-7 and CCL19-secreting CAR-T cell therapy for tumors with positive glypican-3 or mesothelin. *J Hematol Oncol*. 2021;14(1):118. doi:10.1186/s13045-021-01128-9
18. Arvanitakis K, Mitroulis I, Germanidis G. Tumor-associated neutrophils in hepatocellular carcinoma pathogenesis, prognosis, and therapy. *Cancers*. 2021;13(12):2899. doi:10.3390/cancers13122899
19. Haber PK, Castet F, Torres-Martin M, et al. Molecular markers of response to Anti-PD1 therapy in advanced hepatocellular carcinoma. *Gastroenterology*. 2023;164(1):72–88.e18. doi:10.1053/j.gastro.2022.09.005
20. Moreno Ayala MA, Campbell TF, Zhang C, et al. CXCR3 expression in regulatory T cells drives interactions with type I dendritic cells in tumors to restrict CD8(+) T cell antitumor immunity. *Immunity*. 2023;56(7):1613–1630.e1615. doi:10.1016/j.immuni.2023.06.003
21. Wang S, Wu Q, Chen T, et al. Blocking CD47 promotes antitumour immunity through CD103(+) dendritic cell-NK cell axis in murine hepatocellular carcinoma model. *J Hepatol*. 2022;77(2):467–478. doi:10.1016/j.jhep.2022.03.011
22. Bill R, Wirapati P, Messemaker M, et al. CXCL9:SPP1 macrophage polarity identifies a network of cellular programs that control human cancers. *Science*. 2023;381(6657):515–524. doi:10.1126/science.ade2292
23. Zhou SL, Dai Z, Zhou ZJ, et al. Overexpression of CXCL5 mediates neutrophil infiltration and indicates poor prognosis for hepatocellular carcinoma. *Hepatology*. 2012;56(6):2242–2254. doi:10.1002/hep.25907
24. Eruslanov EB, Bhojnagarwala PS, Quatromoni JG, et al. Tumor-associated neutrophils stimulate T cell responses in early-stage human lung cancer. *J Clin Invest*. 2014;124(12):5466–5480. doi:10.1172/JCI77053

25. Tokunaga R, Zhang W, Naseem M, et al. CXCL9, CXCL10, CXCL11/CXCR3 axis for immune activation - A target for novel cancer therapy. *Cancer Treat Rev*. 2018;63:40–47. doi:10.1016/j.ctrv.2017.11.007
26. Chung JY-F, Tang PC-T, Chan M-K-K, et al. Smad3 is essential for polarization of tumor-associated neutrophils in non-small cell lung carcinoma. *Nat Commun*. 2023;14(1):1794. doi:10.1038/s41467-023-37515-8
27. Kim HD, Song GW, Park S, et al. Association between expression level of PD1 by tumor-infiltrating CD8(+) T cells and features of hepatocellular carcinoma. *Gastroenterology*. 2018;155(6):1936–1950.e1917. doi:10.1053/j.gastro.2018.08.030
28. Shi J, Liu J, Tu X, et al. Single-cell immune signature for detecting early-stage HCC and early assessing anti-PD-1 immunotherapy efficacy. *J Immunother Cancer*. 2022;10(1):e003133. doi:10.1136/jitc-2021-003133
29. Lee JY, Nguyen B, Mukhopadhyay A, et al. Amplification of the CXCR3/CXCL9 axis via intratumoral electroporation of plasmid CXCL9 synergizes with plasmid IL-12 therapy to elicit robust anti-tumor immunity. *Mol Ther Oncolytics*. 2022;25:174–188. doi:10.1016/j.omto.2022.04.005
30. Han X, Wang Y, Sun J, et al. Role of CXCR3 signaling in response to anti-PD-1 therapy. *EBioMedicine*. 2019;48:169–177. doi:10.1016/j.ebiom.2019.08.067
31. Wang BL, Tian L, Gao XH, et al. Dynamic change of the systemic immune inflammation index predicts the prognosis of patients with hepatocellular carcinoma after curative resection. *Clin Chem Lab Med*. 2016;54(12):1963–1969. doi:10.1515/cclm-2015-1191
32. Schobert IT, Savic LJ, Chapiro J, et al. Neutrophil-to-lymphocyte and platelet-to-lymphocyte ratios as predictors of tumor response in hepatocellular carcinoma after DEB-TACE. *Eur Radiol*. 2020;30(10):5663–5673. doi:10.1007/s00330-020-06931-5
33. Hu B, Yang XR, Xu Y, et al. Systemic immune-inflammation index predicts prognosis of patients after curative resection for hepatocellular carcinoma. *Clin Cancer Res*. 2014;20(23):6212–6222. doi:10.1158/1078-0432.CCR-14-0442
34. Huang H, Zhang H, Onuma AE, Tsung A. Neutrophil elastase and neutrophil extracellular traps in the tumor microenvironment. *Adv Exp Med Biol*. 2020;1263:13–23.
35. Rovati G, Contursi A, Bruno A, Tacconelli S, Ballerini P, Patrignani P. Antiplatelet agents affecting GPCR signaling implicated in tumor metastasis. *Cells*. 2022;11(4):725. doi:10.3390/cells11040725
36. Solis-Castillo LA, Garcia-Romo GS, Diaz-Rodriguez A, et al. Tumor-infiltrating regulatory T cells, CD8/Treg ratio, and cancer stem cells are correlated with lymph node metastasis in patients with early breast cancer. *Breast Cancer*. 2020;27(5):837–849. doi:10.1007/s12282-020-01079-y
37. Matlung HL, Babes L, Zhao XW, et al. Neutrophils kill antibody-opsonized cancer cells by trogoptosis. *Cell Rep*. 2018;23(13):3946–3959.e3946. doi:10.1016/j.celrep.2018.05.082
38. Zhou SL, Zhou ZJ, Hu ZQ, et al. Tumor-associated neutrophils recruit macrophages and T-Regulatory cells to promote progression of hepatocellular carcinoma and resistance to sorafenib. *Gastroenterology*. 2016;150(7):1646–1658.e1617. doi:10.1053/j.gastro.2016.02.040
39. Patel S, Fu S, Mastio J, et al. Unique pattern of neutrophil migration and function during tumor progression. *Nat Immunol*. 2018;19(11):1236–1247. doi:10.1038/s41590-018-0229-5
40. Leslie J, Mackey JBG, Jamieson T, et al. CXCR2 inhibition enables NASH-HCC immunotherapy. *Gut*. 2022;71(10):2093–2106. doi:10.1136/gutjnl-2021-326259
41. Wang Y, Zhao Q, Zhao B, et al. Remodeling tumor-associated neutrophils to enhance dendritic cell-based HCC neoantigen nano-vaccine efficiency. *Adv Sci*. 2022;9(11):e2105631. doi:10.1002/advs.202105631
42. Song M, He J, Pan QZ, et al. Cancer-associated fibroblast-mediated cellular crosstalk supports hepatocellular carcinoma progression. *Hepatology*. 2021;73(5):1717–1735. doi:10.1002/hep.31792